SCHOOL OF CIVIL ENGINEERING

JOINT HIGHWAY RESEARCH PROJECT

JHRP-74-2

PORE SIZES AND STRENGTH OF A COMPACTED CLAY

Syed Ahmed
C. W. Lovell, Jr.
Sidney Diamond

PURDUE UNIVERSITY
INDIANA STATE HIGHWAY COMMISSION

Technical Paper

PORE SIZES AND STRENGTH OF A COMPACTED CLAY

TO: J. F. McLaughlin, Director
Joint Highway Research Project

February 19, 1974

Project: C-36-5H

FROM: H. L. Michael, Associate Director
Joint Highway Research Project

File: 6-6-8

The attached Technical Paper "Pore Sizes and Strength of a Compacted Clay", has been authored by Syed Ahmed, formerly a Graduate Assistant on our staff, and C. W. Lovell, Jr., and Sidney Diamond, members of our professional staff. The paper presents material previously reported in Interim Report, JHRP, Number 16, September 1971 and titled "Pore Size Distribution and Its Effect on the Behavior of a Compacted Clay".

The paper has been accepted for publication in the ASCE Journal of the Soil Mechanics and Foundation Division (Geotechnical Engineering Division). As it is from an accepted report of the pertinent FHWA Research Project, copies will be sent to FHWA and ISHC for information. It is submitted to the JHRP Board for information and approval of the publication indicated.

Respectfully submitted,

Harold L. Michael
Associate Director

HLM:ms

cc:
W. L. Dolch
R. L. Eskew
G. D. Gibson
W. H. Goetz
M. J. Gutzwiller
G. K. Hallock
M. L. Hayes
C. W. Lovell
G. W. Marks
R. D. Miles
G. T. Satterly
C. F. Scholer
M. B. Scott
J. A. Spooner
H. R. J. Walsh
E. J. Yoder
S. R. Yoder

TECHNICAL REPORT STANDARD TITLE PAGE

1. Report No.	2. Government Accession No.	3. Recipient's Catalog No.

4. Title and Subtitle	5. Report Date
PORE SIZES AND STRENGTH OF A COMPACTED CLAY	February 1974
	6. Performing Organization Code: C-36--H

7. Author(s)	8. Performing Organization Report No.
Syed Ahmed, C. W. Lovell, Jr., Sidney Diamond	JHRP-2-74

9. Performing Organization Name and Address	10. Work Unit No.
Joint Highway Research Project Civil Engineering Building Purdue University West Lafayette, Indiana 47907	11. Contract or Grant No.: HPR-1(10) Part II
	13. Type of Report and Period Covered: Technical Paper
12. Sponsoring Agency Name and Address Indiana State Highway Commission State Office Building 100 North Senate Avenue Indianapolis, Indiana 46204	14. Sponsoring Agency Code: CA 370

15. Supplementary Notes

Conducted in cooperation with the U.S. Dept. of Transp. Federal Highway Admin. Research study titled "Pore Size Distribution and Its Effect on the Behavior of Compacted Clayey Soils".

16. Abstract

Pore size distributions of a compacted commercial clay were measured by mercury intrusion, following removal of the soil water by freeze drying. These distributions were related to variables of compaction water content, method of laboratory compaction, and unconfined compressive strength.

17. Key Words	18. Distribution Statement
Clay; Compaction; Freeze Drying; Microstructure; Pore Sizes; Shrinkage; Soil Properties; Strength; Sublimation	

19. Security Classif. (of this report)	20. Security Classif. (of this page)	21. No. of Pages	22. Price
Unclassified	Unclassified	42	

Form DOT F 1700.7 (8-69)

Technical Paper

PORE SIZES AND STRENGTH OF A COMPACTED CLAY

by

Syed Ahmed

C. W. Lovell, Jr.

Sidney Diamond

Joint Highway Research Project

Project No.: C-36-5H

File No.: 6-6-8

Prepared as Part of an Investigation
Conducted by

Joint Highway Research Project
Engineering Experiment Station
Purdue University

in cooperation with the

Indiana State Highway Commission

and the

U.S. Department of Transportation
Federal Highway Administration

Purdue University
West Lafayette, Indiana
February 19, 1974

KEY WORDS: clay; compaction; freeze drying; microstructure; pore sizes; shrinkage; soil properties; strength, sublimation.

SUMMARY

Pore size distributions of a compacted commercial clay were measured by mercury intrusion, following removal of the soil water by freeze drying. These distributions were related to variables of compaction water content, method of laboratory compaction, and unconfined compressive strength.

List of Figure Captions

Caption

Fig.

List of Table Captions

Caption

Table

ABSTRACT

In a series of laboratory investigations, pore size distributions, compaction characteristics, and undrained strength and deformation data were related to molding water content and type of laboratory compaction. The soil used was the commercially available illite clay called Grundite.

Pore size distribution measurements, carried out by mercury porosimetry, require dry samples. Conventional oven drying is unsuitable, since the distribution may be modified by the shrinkage caused by evaporative drying. Removal of the water with small to negligible volume change is possible by freeze drying, and suitable equipment and techniques for this process were developed.

The pore size distribution measurements were obtained, after freeze drying, for a diameter range of about 600 μm to about 0.016 μm. The results indicate a strong influence of the molding water content, but only a minor influence of the method of compacting to a given moisture-unit weight condition.

Samples compacted at moisture contents less than the Proctor optimum moisture content showed brittle compressive failures at low strains, apparently due in part to the breakdown of numerous larger pores. Samples compacted wet of optimum continued to deform to high strains.

PORE SIZES AND STRENGTH OF A COMPACTED CLAY

By Syed Ahmed,[1] A.M. ASCE; Charles William Lovell, Jr.,[2] F. ASCE; and Sidney Diamond[3]

INTRODUCTION

Clayey soils find frequent use in compacted highway subgrades and embankments. The load deformation and water transmission characteristics of these compacted clays are recognized to be dependent upon the packing and arrangement of the particulate units (4, 5).[4] Measured values of these characteristics are affected by the bulk porosity (or average unit weight), and these in turn afford many useful correlations with performance. A particular unit weight can be achieved with a variety of particulate arrangements, so that correlation with soil characteristics should improve when soil structure or fabric can also be taken into account (10).

The examination of the distribution of non-solid space also may add significantly to understanding and prediction of soil behavior. It is logical to approach this aspect of soil fabric by the measurement of pore size distributions that result from application of different levels of moisture content, compactive effort, and compactive type.

---

1. Soils Engineer, Harza Engineering Company, Chicago, Illinois.
2. Professor, School of Civil Engineering, Purdue University, West Lafayette, Indiana.
3. Professor, School of Civil Engineering, Purdue University, West Lafayette, Indiana.
4. Numerals refer to items in Appendix I-References.

One can then presumably correlate changes in pore size distribution with changes in dependent variables like compacted unit weight, strength, stiffness, and the like.

Thus, the independent variables selected for examination in this study were the method of compaction, the compactive effort, and the molding water content. Only one clay was used, the commercially available Grundite, but a pilot study conducted on Georgia kaolinite and Leda clay showed that corresponding relationships can be obtained for other soils as well. See Figure 1 for the cumulative grain size distribution of the Grundite. Three methods of compaction, viz., impact (Standard Proctor), kneading, and static were used. The compactive effort level was held constant for the Standard Proctor compaction. For other compactive types, the energy applied at each selected moisture content was varied to produce the predetermined unit weight given by the Standard Proctor compaction result for that moisture content. Water contents were chosen to cover the practical range of laboratory compaction.

Undrained, unconfined stress-strain and strength characteristics of the compacted soils were also investigated, since they are descriptive of the engineering performance of the soil in the "as-compacted" condition.

Pore size distributions were obtained by mercury porosimetry. A review of previous experience with this procedure gave a preliminary indication of its suitability for this research. Its successful use with soils has been reported by Diamond (2), Sridharan (12) and Sridharan et. al. (13), among others. Although for the compacted

illite clays studied in this work only about eighty percent of the total pore space could be penetrated by the available equipment of 15,000 psi (1033×10^5 N/m^2) pressuring capacity, pores varying in diameter over five orders of magnitude (600 μm to about 0.016 μm) were measured. Comparisons among pore size distributions have been made principally by the relative shapes and positions of cumulative frequency distribution curves.

An essential requirement for measuring the sizes of the pores is that the pores not contain water. However, in conventional oven or air drying, the surface tension force exerted on the structure by the pore water increases progressively as the menisci become more curved; in consequence, the sample usually shrinks, with some modification of the interparticle arrangement. Constant volume drying is desired, and a freeze-dry technique was selected to approximate this. In the freezing step, the cooling rate must be very rapid to minimize moisture migration under gradients induced in the vicinity of ice nucleation (3, 6, 7). The samples used in this research were small, and were rapidly cooled in liquid nitrogen at about -196C (77K). The frozen moisture was then removed by sublimation, hopefully without significant volume change.

PREPARATION OF SAMPLES

Compaction

Three compactive types were used: impact, kneading, and static.

Impact Compaction The Standard Proctor compaction procedure, a widely used standard test, was used. In the present study, once the compaction curve had been established, four standard compaction moisture

contents were selected, viz., one somewhat dry of the optimum, one slightly drier than optimum, one approximately equal to the optimum, and one distinctly wet of optimum. For much of the later work, the second of these was not used.

Kneading Compaction The compaction procedure developed by Wilson (13) and known as "Harvard Miniature Compaction" was used, with the exception that manual tamping was replaced by mechanical tamping. At each of the standard moisture contents, samples were prepared with the compaction effort adjusted by changing the number of tamps and the tamping pressure, in order to produce the unit weight corresponding to that observed with Standard Proctor compaction for the same moisture content.

Static Compaction The static procedure is not standardized and can be implemented in a variety of ways; but a major problem often observed is severe non-uniformity of local unit weight attained in different parts of the sample. To minimize this problem, the technique described by Sridharan (12) was employed. A 2 inch (5.08 cm) high mold was used, which has an inside diameter of 1 inch (2.54 cm). Six extension pieces were employed. Compaction was carried out in six stages, with an extension piece being removed after each stage. Here again, the effort was varied to permit attainment of a unit weight at each moisture content identical to that obtained by the Standard Proctor method for that moisture content.

Most of the compacted soils were sampled using a miniature tube sampler specially designed for this purpose. A teflon-tipped extruder was used to remove the soil from the tube. The sampling and extrusion procedure worked well for samples compacted near, at, or above the moisture content corresponding to Standard Proctor optimum. Drier

materials were found to be best sampled by cutting out small roughly cubical specimens with a sharp razor blade.

It was found that, in general, the porosity of the specimens varied somewhat with the position in the compacted sample, especially for the Standard Proctor samples. Unfortunately it was quite impossible to measure the total porosity of the small specimens to the degree of precision desired, with the means at hand.

Freeze Drying

Freeze drying is a batch process, involving rapid freezing of samples in the liquid nitrogen, transfer to a sublimation unit, and finally sublimation (8, 9).

For freezing, the samples were held in buckets which consisted of a porous stone base and walls made of aluminum foil, forming several individual compartments. The buckets were rapidly lowered into liqud nitrogen which reached the specimens simultaneously from all sides. Freezing was accompanied by a bubbling induced by the loss of heat from the samples.

After freezing, the specimens were transferred to a four-bay sublimation unit which is shown in Figure 2. The unit consists of a glass sample container surrounded by a slush contained in a Dewar flask. The sample container is connected by glass tubing to a condensing liquid. On the top are stopcocks which connect the bays with the vacuum pump. Bleeder valves are also provided for introducing air. The whole assembly is mounted on a rigid frame.

The sublimation process was carried out in the following manner. An ice-water slush was placed in a Dewar flask and the glass sample container was placed in it. After the container had achieved temperature

equilibrium with the slush, the frozen samples were placed within it. The temperature of the slush was maintained low enough to insure that the samples remain frozen during the sublimation process. The container was then connected to the condenser, and a Dewar filled with liquid nitrogen was positioned so as to chill the condensing tube. The timing of these actions was critical, viz., positioning of the liquid nitrogen Dewar must immediately follow the connecting of the sample container to the apparatus, or, moisture may condense in the sample container or on the samples. Next, a vacuum was applied by opening the stopcock of the bay, and finally, the bleeder valve was closed and sublimation allowed to proceed.

A slush bath was required which could provide a temperature low enough to keep all soil water frozen, but high enough to produce a vapor pressure resulting in drying in a reasonable span of time. Two baths were finally chosen. The first was prepared by partially freezing m-Xylene with liquid nitrogen; this gave a temperature in the vicinity of -40C (233 K). The second was prepared by mixing magnesium chloride with crushed ice; this gave a temperature of about -21C (252 K). However, this latter temperature rose quickly due to the melting of ice and it was necessary to continue to add chunks of dry ice to compensate for the melting, which maintained the bath between the temperatures of -24 to -30C (249 K to 243 K) for a number of hours. Both of these slush baths were reasonably satisfactory, but not completely so. Xylene is flammable; $MgCl_2$ is messy, but less hazardous.

The frozen samples were dried in a period of 12 to 18 hours. The slush bath was then removed and an equilibration period of a few hours was allowed before the samples were finally removed from the apparatus. Sample weights before and after freeze drying were recorded to determine

the amount of water removed. Micrometer measurements of selected samples showed small reductions in the bulk volume, and hence in the porosity resulting from the freeze-drying processes. These measurements were only partially reproducible, but it was concluded from them that the shrinkage incurred during freeze drying was small, and hopefully negligible.[1]

MEASUREMENT OF PORE SIZES

Pore size distribution measurements were carried out as described by Diamond (2). The equipment used was a modified Aminco-Winslow mercury porosimeter generating a maximum of 15,000 psi (1033×10^5 N/m^2) pressure by means of a motor-driven hydraulic pump. Pores in the diameter range from about 600 μm to about 16 μm were measured first, using a separate horizontal filling device similar to that now commercially available under the designation "Aminco-Macroporosimeter"[2] The contact angle assumed in the calculations was that found for illite by Diamond, 147°. Sample sizes were of the order of 0.5 to 1 gm.

Briefly, the experimental procedure was as follows. The sample was placed in the penetrometer and weighed. It was then placed in the filling device and evacuated to such a low pressure that the empty space in the penetrometer could be filled with mercury. After filling

---

1. The exact magnitude of shrinkage under freeze drying is still under investigation (1973).

2. American Instrument Co., Division of Travenol Laboratories, Silver Spring, Md.

the penetrometer, pressure was raised in an stepwise fashion, and intrusion of mercury into the voids was read on the stem of the penetrometer. When the pressure had been raised to the atmospheric pressure, the mercury filled penetrometer was taken out of the filling device and weighed again. Subsequently it was placed in the porosimeter, to obtain the sizes of the voids which are not penetrable at one atmosphere pressure. In the porosimeter the void penetration is displayed on a digital readout along with applied pressure. For a detailed description of the apparatus, its limitations, and its use, the reader is referred to Winslow and Diamond (14), and Sridharan et al (12).

RESULTS

Cumulative Pore Size Distribution

It was found that replicate pore-size distribution curves from small specimens sampled from various regions within a compacted sample, while very similar in most characteristics, were not identical, especially with respect to the content of the largest pores measured. It is thought that most of this variation is a reflection of the inherent variation in local bulk density, as has been demonstrated to exist by Schackel (11), although some of it is due to instrumental problems.

In general, the results of a series of supposedly replicate pore size distribution determinations yield a band. A typical example is shown in Figure 3, which illustrates the results obtained for five replicate specimens sampled from a soil compacted by the Standard Proctor method at optimum moisture content.

Clearly, some method of averaging these individual results is required. The method chosen, while arbitrary, seems to be satisfactory.

To obtain an averaged cumulative curve from such a band, each curve was subdivided into an identical number of short segments, the number of such ranging from 21 to 32, depending on the characteristics of the overall band. Within each segment, the increase in volume penetrated by mercury, "Δ penetration", was calculated as the curve advanced from the upper diameter to the lower diameter bound of the segment. The "Δ penetration" was calculated separately for each replicate and averaged to give the average increase in volume penetrated for the segment. The average cumulative pore size distribution was obtained by adding the results for successive segments. Figure 4 illustrates the characteristics of such an averaged pore size distribution curve, and represents the average compiled from the five replicate curves of Figure 3.

The maximum diameter pore tallied in these measurements is limited by the pressure used to effect the filling of the penetrometer with mercury, which was 20 mm. Hg. (26.7×10^2 N/m^2). This limited the largest measureable pore diameter to approximately 600 micrometers. The smallest diameter measured, limited by the pressuring capacity of the porosimeter, was about 160 Å. Application of this maximum pressure resulted in filling (and tallying) only about eighty percent of the void space calculated to be present from the specific gravity and dry unit weights of the samples. Nevertheless, the experimental distributions cover about five orders of magnitude of pore diameter. Most of the remaining pore volume is thought to be in pores finer than 160 Å in diameter.

Effect of Molding Water Content

Average cumulative pore size distribution curves are plotted in Figures 5, 6, and 7 for the Standard Proctor, kneading, and static

compactions at four different molding water contents. These water contents are "dry", "near optimum", "optimum", and "wet of optimum", as defined with reference to the Standard Proctor curve. Certain soil descriptors are shown in Table 1, where it is also observed that the "wet" and "dry" points have the same total porosity. However, it is seen from the above figures that the distribution of the porosity for the two moisture conditions is sharply different. The distribution of pore sizes seems to be affected by as little as a 2% difference in water content, even though the total calculated porosity does not change more than 0.02 cm^3/gm. For example, compare the distribution for the "near optimum" and "optimum" water contents in Figure 5.

It is convenient to study these curves in terms of three arbitrary diameter ranges: "coarse", from 600 μm to 50 μm; "medium", 50 μm to 0.5 μm; and "fine", 0.5 μm to 0.016 μm. These limits are different from those considered appropriate for describing the statically compacted kaolinite studied earlier by Sridharan et. al. (13).

It is found that the pore size distribution curves of the samples compacted by different methods, but at the same molding water content and to the same dry unit weight show similar characteristics. The observations that follow thus apply to the results obtained with all the methods of compaction.

The pore size distribution curves for the dry side compaction show that only a small percentage of the total porosity, of the order of about 7%, is present in the coarse range. The curves for such samples take a sharp upturn as they enter the arbitrarily defined medium pore range at about 50 μm, and a large percentage of total porosity, of the order of 40%, lies in this range. Intruded porosity in the arbitrarily defined fine range (less than 0.5 μm) is about 27% of the total.

Pore size distribution curves for the samples compacted near optimum are somewhat different. Although they also show only a small percentage of the total porosity (of the order of 13%) in the coarse pores, the porosity in the medium range drops to about 19%, and in the fine range rises to 49% of the total porosity. As the molding water content is increased to optimum, quite similar values of 9%, 17%, and 49% of the total porosity are obtained for the coarse, medium, and fine ranges of the pore diameters, respectively. It should be noted that the percentage of the total porosity which was penetrable was almost the same for samples compacted at the different molding water contents, being 78, 81, 76, and 79 for the dry, near optimum, at optimum, and wet of optimum, respectively. Despite this, slight differences in molding water content result in measurable changes in the pore size distribution. This sensitivity of the measured distribution to molding water content is clearly shown by the differences in the curves for near-optimum and at-optimum compaction, for every method of compaction used in this study.

In the examination of the pore size distribution curves for the samples compacted wet of optimum, values of the order of 7%, 19%, and 53% of the total porosity are obtained for the arbitrarily defined coarse, medium, and fine ranges of diameter. The percentage for the coarse range is about the same as was obtained for the samples compacted dry of optimum, but the percentage for the medium range is slightly less than half that obtained for the dry side samples, and the percentage for the fine range is about twice that obtained for the dry side samples. As noted before, the samples on the dry and

the wet side were compacted to the same porosity, yet the distribution of porosity among the different sizes of the pores is markedly different.

Effect of Kind of Compaction

The average cumulative curves of Figures 8, 9 and 10 compare pore size distributions with essentially constant moisture and total porosity but for different methods of compaction. The differential effect of the method of compaction is seen to be unimportant. In fact, the band width of these average cumulative pore size distribution curves for the various methods of compaction at any one water content is comparable to that for replicate samples prepared by the same method of compaction.

Numerical representations of the cumulative pore size distributions are helpful in interpretation. The simplest of such representations is the mean pore diameter. An average porosity was obtained from the values of porosity for the different methods of compaction at a particular water content. The mean diameter (D_{50}) was defined as the diameter obtained at 50% of this porosity on the assumption that pores not tallied are too small to be intruded at the maximum pressure available. Relative values of D_{50} are plotted in Figure 11. The values of D_{50} are similar for all compaction methods for samples compacted on the wet side and at optimum, but are quite different for dry side compaction. Both kneading and static compaction yield larger average pore diameters for such samples than does Standard Proctor compaction.

Effect of Method of Drying

Pore size distributions obtained using specimens dewatered by conventional (oven) drying were studied to compare them with those obtained after freeze drying. Curves for the oven-dried specimens are shown as solid lines, and curves for the corresponding freeze-dried specimens are shown as dashed lines in Figures 12, 13 and 14. It appears that the initial molding water content is significant in these comparisons. Specimens compacted wet of optimum and dried in the oven showed a considerable reduction in the total porosity as compared with similar specimens dewatered by freeze drying. Figure 12 is specifically for Standard Proctor compaction, but the static and kneading curves are quite similar. Pore size distribution curves obtained after oven drying for these wet-of-optimum samples show far less pore volume in sizes ranging from about 5 to 0.1 μm than do the curves obtained after freeze drying. Below 0.1 μm the curves are similar. Oven drying of clays from high degrees of saturation would be expected to produce high shrinkage, and it appears that pores of the 5 to 0.1 μm size range are most drastically affected.

Oven-dried samples compacted at optimum water content also showed reduced porosity compared to freeze dried samples, but the differences are much smaller. However, here there is a distinct effect of the kind of compaction. For both kneading and static compaction, the two curves representing oven and freeze-dried specimens are almost parallel, i.e., they show a rather uniform reduction in porosity. However, as shown in Figure 13, the two curves for the Standard Proctor

compaction are identical except for a reduction in volume of pores between about 0.5 and 0.1 μm in diameter displayed by the oven-dried specimens.

The dry side samples had a low degree of saturation (about 46%) and presumably the highest pore water tensions. As oven drying takes place, the water tension presumably increases, but also acts over smaller areas. The net result of oven drying for such samples is only a small shrinkage or sometimes even an expansion or relaxation. The resulting oven dry porosity may be comparable to that obtained after freeze drying, or it may even be slightly greater than that obtained after freezing drying. The pore size distribution curves for the dry side Standard Proctor compaction (Figure 14) suggest that the latter is true here. Corresponding results for kneading and static compaction show porosities after oven drying which are very slightly less than after freeze drying (1). Thus, at low degrees of saturation, it appears that oven drying may accomplish dewatering without gross changes in the as-compacted structure.

Strength and Deformation Characteristics

Unconfined compression tests were run in a triaxial cell at a constant rate of strain. See Reference 1 for testing details.

Samples compacted by static compaction were of appropriate size [1.31 in. dia. by 2.62 in. (3.33 cm by 6.65 cm.)] for the unconfined compression testing. Samples compacted by kneading compaction were cut to size using a miter box. The cylinders compacted by Standard Proctor procedure were divided into four quarters by a metal band saw. A specially fabricated steel cylinder was used to hold the cylinder while sawing. The quarters of the cylinder were finally cut and shaped by an electrically driven soil lathe.

Table 2 summarizes the values of the peak stresses and the corresponding axial strains for all compactive types. The reduction of axial load to axial stress was usually based upon the measured sample diameter at mid-height (1). Wherever actual diameter measurements were not available, the stress was calculated using the constant volume assumption. Pore pressures were not measured. Initial corrections were applied to the stress-strain curves where needed.

The stress-strain curves for the dry side compaction are characterized by brittle failure at low strains (1). Pore size distribution studies of these samples revealed that the medium pore size class (50 μm to 0.5 μm diameter) was dominant. For such samples the axial stress dropped off sharply past the peak, and the samples fragmented rather completely. Samples compacted at the Standard Proctor optimum were stronger and had higher failure strains; they densified to failure. The wet side samples showed less densification due to shear, and they had the lowest strengths and the highest failure strains (1). For both the optimum and wet side samples the fine pore fractions are dominant. Although the dry side and the wet side samples were compacted at moisture contents about the same percentage of water distant from the optimum, the samples on the wet side were both less strong and less stiff.

It is interesting to compare the average relative dry unit weight and the average relative peak stress obtained for specimens compacted by all the different method of compaction at given molding water contents. Average dry unit weight for the dry side compaction point was about 95% of the dry unit weight at optimum, and that for the wet side

compaction point was about 96% of the dry unit weight at optimum (1). On the other hand, the peak stresses were about 76% and 54% of the peak stress recorded for samples compacted at optimum for the dry side and wet side compactions, respectively. These substantial differences in the peak stresses of specimens prepared by dry side and wet side compaction are undoubtedly related to the differences in the distribution of pore sizes. However, since other important factors, including pore pressures and other aspects of soil fabric, are also operative, it is not possible to assess the specific influence of pore size unambiguously.

CONCLUSIONS

1. For three different methods of compaction carried out in such a way as to follow a common moisture-density curve, the pore size distribution of a compacted illite clay after freeze drying has been found to depend most strongly on the compaction moisture content. The effect of varying moisture content is found primarily in the distribution of pores smaller than 50 μm.

The features of the pore size distribution become more distinct when they are divided arbitrarily into three pore diameter ranges: "coarse", from 600 to 50 μm; "medium", 50 to 0.5 μm; and "fine", 0.5 to 0.016 μm. For all methods of compaction, more than 40% of the total porosity is in the medium pore diameter range when the samples are compacted at moisture contents dry of Proctor Standard optimum. At optimum and wet of Proctor optimum the distributions are finer, half or more of the total porosity being in the fine range. Samples compacted on the wet side of Proctor optimum possess twice as much porosity in the fine range as dry side samples with the same total porosity.

2. The method of compaction affected the pore size distribution of the compacted illite clay very little, at least under the imposed constraint that samples were compacted to the same moisture-unit weight conditions by each of the different methods of compaction.

3. Stress-strain curves measured in unconfined compression for the compacted illite clay varied systematically with molding water content. For samples compacted and tested dry of Proctor optimum, brittle failures occurred at low axial strains. Quasi-brittle failures at moderate strains were observed for samples compacted at Proctor optimum. Gradual shear failure at high strains occurred for the wet side compaction samples. The highest peak strength [71 psi ($489.5 \times 10^3 N/m^2$)] was recorded for samples compacted in the Standard Proctor test to the Proctor optimum. Samples compacted by kneading compaction on the wet side of Proctor optimum showed the lowest strength [32 psi ($220.6 \times 10^3 N/m^2$)].

On the average, the peak strength of samples compacted on the wet side of Proctor optimum was about two thirds that for samples compacted on the dry side of Proctor optimum. These comparisons are made at equal unit weights.

4. Samples with similar total porosity values can have entirely different pore size distributions. Therefore, pore size distributions can correlate differently with soil behavior than total porosity.

5. Freeze drying of compacted samples is reasonably suitable as a dewatering method for this research, in contrast to oven drying, which induces a shrinkage varying greatly with the degree of saturation. Samples compacted to a high degree of saturation were reduced in volume as much as 20% when oven dried. At low degrees of saturation the

the shrinkage was quite small. At about 50% saturation, the pore size distributions determined after oven drying were substantially the same as those determined after freeze drying.

ACKNOWLEDGMENTS

This research was supported by the Indiana State Highway Commission and the Federal Highway Administration, U. S. Department of Transportation, and was administered through the Joint Highway Research Project, Purdue University.

The freeze-drying equipment was originally designed by Mr. James R. Hooper, presently employed by McClelland Engineers, Inc. of Houston, Texas.

APPENDIX I - REFERENCES

1. Ahmed, Syed: "Pore Size Distribution and its Effect on the Behavior of a Compacted Clay", MSCE Thesis, Purdue University, June 1971, 200 pp. Also: Joint Highway Research Report No. 16, Sept. 1971, Purdue University.

2. Diamond, S.: "Pore Size Distribution in Clays", Clays and Clay Minerals, Vol. 18, 1970, pp. 7-23.

3. Dowell, L. G., and Reinfret, A. P.: "Low Temperature Forms of Ice as Studied by X-Ray Diffraction", Nature, Vol. 188, Dec. 31, 1960, pp. 1144-1148.

4. Lambe, T. W.: "The Engineering Behavior of Compacted Clay", Jour. Soil Mech. and Foundation Div., Paper No. 1654, May, 1958.

5. Lambe, T. W.: "The Engineering Behavior of Compacted Clay", Jour. Soil Mech. and Foundation Div., Paper No. 1655, May, 1958.

6. Luyet, B., Tanner, J. and Rapatz, C.: "Recent Developments in Crystobiology and their Significance in the Study of Freezing and Freeze Drying of Bacteria", Proc. Low Temperature Microbiology Symposium, Camden, N.J., 1961.

7. Merryman, H. T.: "X-Ray Analysis of Rapidly Frozen Gelatin Gels," Biodynamica, Vol. 8, No. 157, Dec. 1958, pp. 69-72.

8. Merryman, H. T.: "Principles of Freeze Drying", New York Academy of Science, Vol. 85, March-May, 1960.

9. Rowe, Terence, W. G.: "The Theory and Practice of Freeze Drying", New York Academy of Sciences Annals, Vol. 85, March-May, 1960.

10. Seed, H. B. and Chan, C. K.: "Structure and Strength Characteristics of Compacted Clays", Jour. Soil Mech. and Foundation Div., Oct. 1959.

11. Shackel, B.: "The Compaction of Uniform, Replicate Soil Specimens", Australian Road Research, Vol. 4, 1970, pp. 12-31.

12. Sridharan, A.: "Some Studies on the Strength of Partly Saturated Clays", Ph. D. Thesis, Purdue University, 1968.

13. Sridharan, A., Altschaeffl, A. G., and Diamond, S.: "Pore Size Distribution Studies", Jour. Soil Mech. and Foundation Div., May 1971.

14. Wilson, S.D.: "Suggested Method of Test for Moisture Density Relations of Soils Using Harvard Compaction Apparatus", Engineering News Record, Nov. 2, 1950.

15. Winslow, D. N. and Diamond S.: "The Pore Size Distribution of Portland Cement Paste", Journal of Materials, Vol. 5, No. 3, 1970.

APPENDIX II. - NOTATION

The following symbols are used in this paper:

D = pore diameter

D_{50} = mean pore diameter

e = void ratio

HM = Harvard miniature (kneading) compaction

n = porosity

OMC = optimum water content in the Standard Proctor compaction test

S = degree of saturation (%)

SP = Standard Proctor compaction

ST = static compaction

w_o = water content (%)

Å = Angstrom

γ_d = dry unit weight

$\mu(\mu m)$ = micron (micrometer)

TABLE 1

PROPERTIES OF THE COMPACTED SAMPLES USED
IN FREEZE DRYING AND PORE SIZE DETERMINATIONS

STANDARD PROCTOR (SP)

Property	Sample No. and Relative Water Content	1 (Dry)	2 (Near Optimum)	3 (Optimum)	4 (Wet)
Water Content (w) %		15.6	20.2	21.5	26.0
Dry Unit Weight (γ_d) pcf		96.0	99.6	100.1	96.4
	(kg/m^3)	(1.54×10^3)	(1.60×10^3)	(1.60×10^3)	(1.54×10^3)
Void Ratio (e)		0.80	0.74	0.73	0.79
Porosity (n) cm^3/gm or m^3/kg		0.29	0.26	0.26	0.29
Degree of Saturation (S) %		54.1	75.9	81.5	91.0

KNEADING COMPACTION (HM)

Property	Sample No. and Relative Water Content	1 (Dry)	2 (Near Optimum)	3 (Optimum)	4 (Wet)
Water Content (w) %		16.2	19.8	21.4	26.2
Dry Unit Weight (γ_d) pcf		96.0	102.7	99.5	96.3
	(kg/m^3)	(1.54×10^3)	(1.64×10^3)	(1.59×10^3)	(1.54×10^3)
Void Ratio (e)		0.80	0.68	0.74	0.80
Porosity (n) cm^3/gm or m^3kg		0.29	0.25	0.27	0.29
Degree of Saturation (S) %		55.9	80.0	80.0	90.1
Pressure on Tamper lbs		39.5	39.5	30.7	21.9
	(N)	(176)	(176)	(137)	(97)
No. of Tamps for each of five layers		13	10	15	20

STATIC COMPACTION (ST)

Property	Sample No. and Relative Water Content	1 (Dry)	2 (Near Optimum)	3 (Optimum)	4 (Wet)
Water Content (w) %		15.6	19.4	21.4	26.1
Dry Unit Weight (γ_d) pcf		96.1	99.8	100.2	96.5
	(kg/m^3)	(1.54×10^3)	(1.60×10^3)	(1.61×10^3)	(1.55×10^3)
Void Ratio (e)		0.80	0.73	0.73	0.79
Porosity (n) cm^3/gm or m^3/kg		0.29	0.27	0.26	0.29
Degree of Saturation (S) %		50.9	72.9	81.5	90.5

COMPARATIVE COMPACTION AND STRENGTH VALUES

Test No.	Compaction Type*	Water Content	Dry Unit Weight pcf (kg/m^3)	Peak Stress (Actual Diameter) psi (N/m^2)	Failure Strain (Actual Diameter) %	Peak Stress (Const. Volume) psi (N/m^2)	Failure Strain (Const. Volume) %
9	SP	15.64 (dry) **	96.0 (1.54×10^3)	-	-	55.3 (38.1×10^4)	4.19
10	HM	16.15 (dry)	95.3 (1.53×10^3)	-	-	51.9 (35.8×10^4)	3.02
14	ST	15.64 (dry)	95.7 (1.53×10^3)	48.1 (33.2×10^4)	2.40	47.2 (32.5×10^4)	2.40
17	ST	15.64 (dry)	96.2 (1.54×10^3)	56.0 (38.6×10^4)	2.88	-	-
7	SP	21.37 (optimum)	100.1 (1.60×10^3)	74.0 (51.0×10^4)	5.41	70.9 (48.9×10^4)	5.41
21	SP	21.37 (optimum)	100.1 (1.60×10^3)	74.1 (51.1×10^4)	5.76	-	-
8	HM	21.43 (optimum)	99.1 (1.59×10^3)	66.3 (45.7×10^4)	5.64	62.8 (43.3×10^4)	5.64
13	ST	21.37 (optimum)	100.2 (1.61×10^3)	-	-	62.3 (43.0×10^4)	4.22
19	ST	21.37 (optimum)	99.7 (1.60×10^3)	64.2 (44.3×10^4)	4.48	-	-
6	SP	26.05 (wet)	96.4 (1.54×10^3)	40.0 (27.6×10^4)	6.40	38.5 (26.5×10^4)	6.40
20	SP	26.05 (wet)	96.4 (1.54×10^3)	37.3 (25.7×10^4)	6.25	-	-
5	HM	26.23 (wet)	96.3 (1.54×10^3)	33.1 (22.8×10^4)	6.86	32.2 (22.2×10^4)	6.36
22	HM	26.23 (wet)	95.9 (1.54×10^3)	30.4 (21.0×10^4)	5.60	-	-
23	HM	26.23 (wet)	96.1 (1.54×10^3)	30.15 (20.8×10^4)	7.24	-	-
11	ST	26.05 (wet)	96.1 (1.54×10^3)	-	-	49.2 (33.9×10^4)	5.74

*SP: Standard Proctor; HM: Kneading Compaction; ST: Static Compaction

**Water content relative to Standard Proctor optimum.

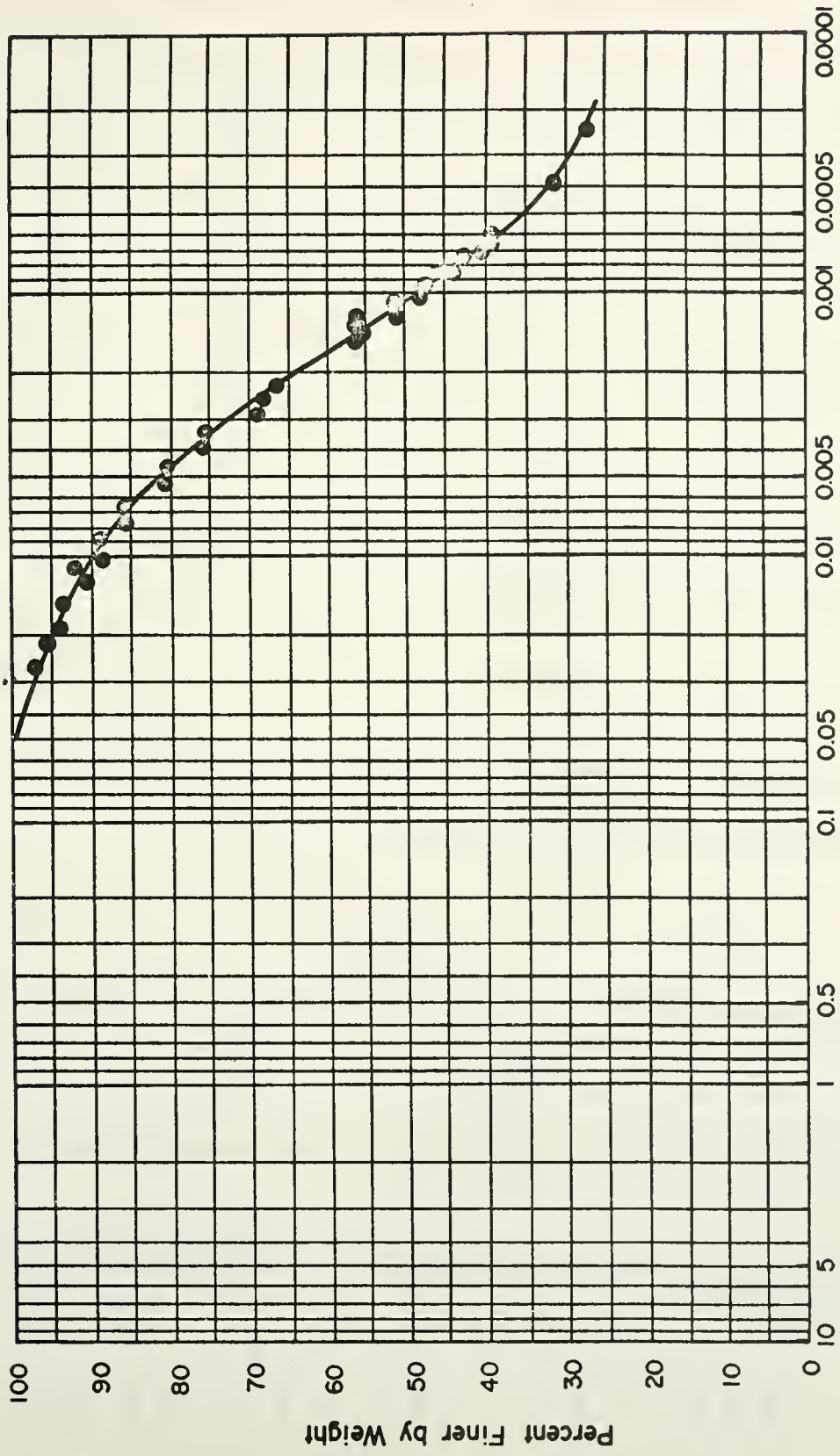

FIGURE 1. GRAIN SIZE DISTRIBUTION FOR GRUNDITE

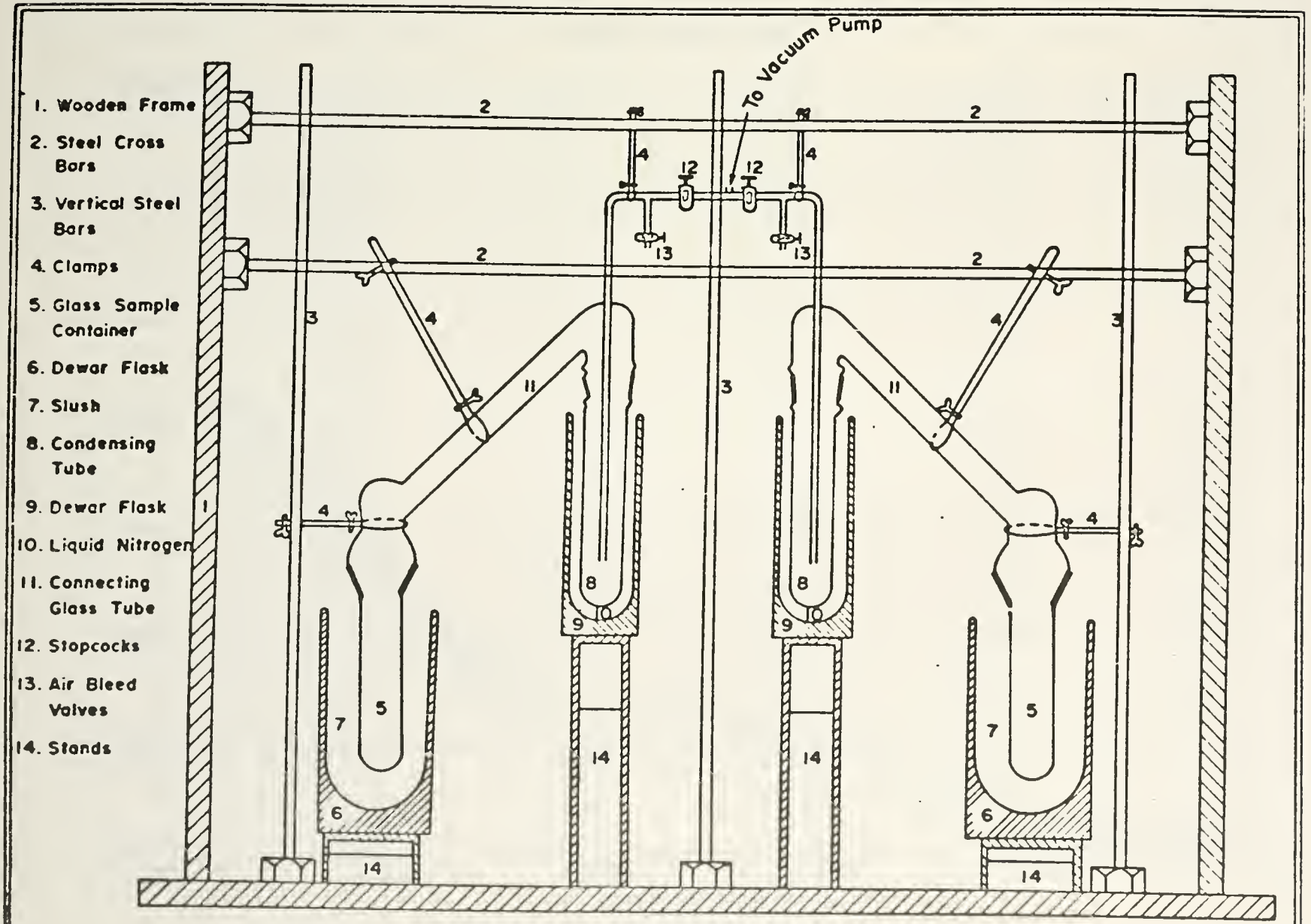

Figure 2. - Sublimation Unit

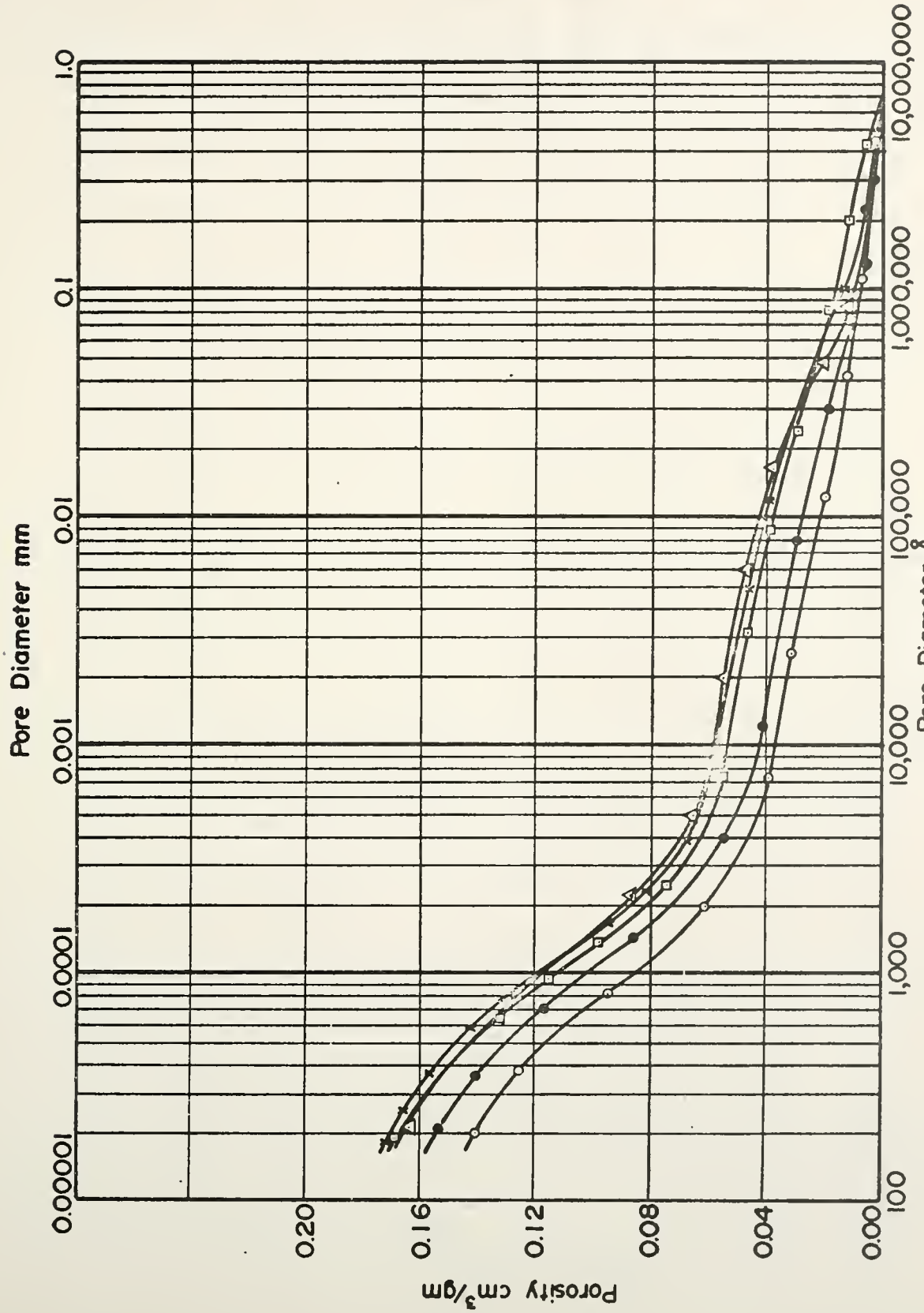

Figure 3. Typical Pore Size Distribution Band

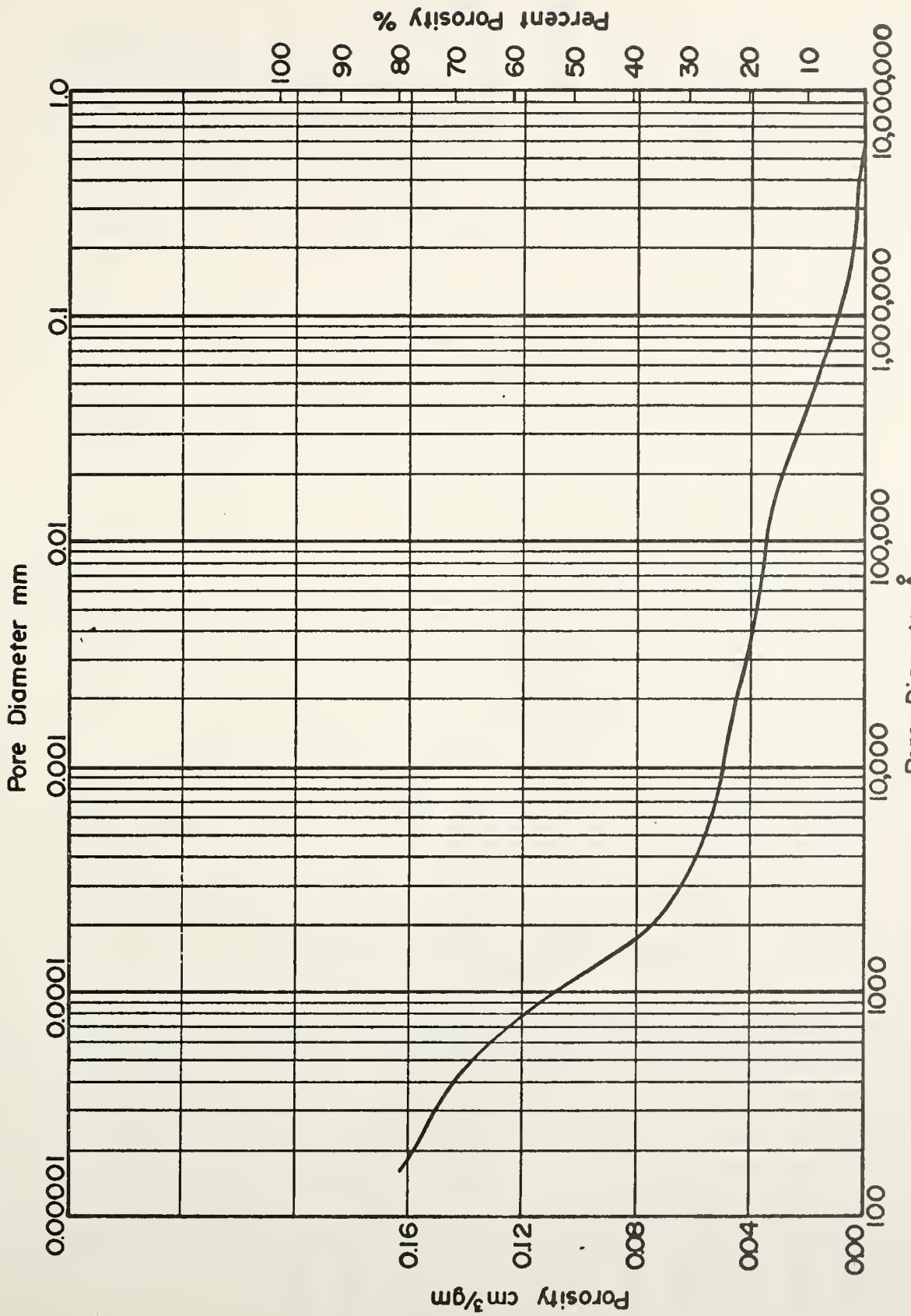

Figure 4. Average Cumulative Pore Size Distribution

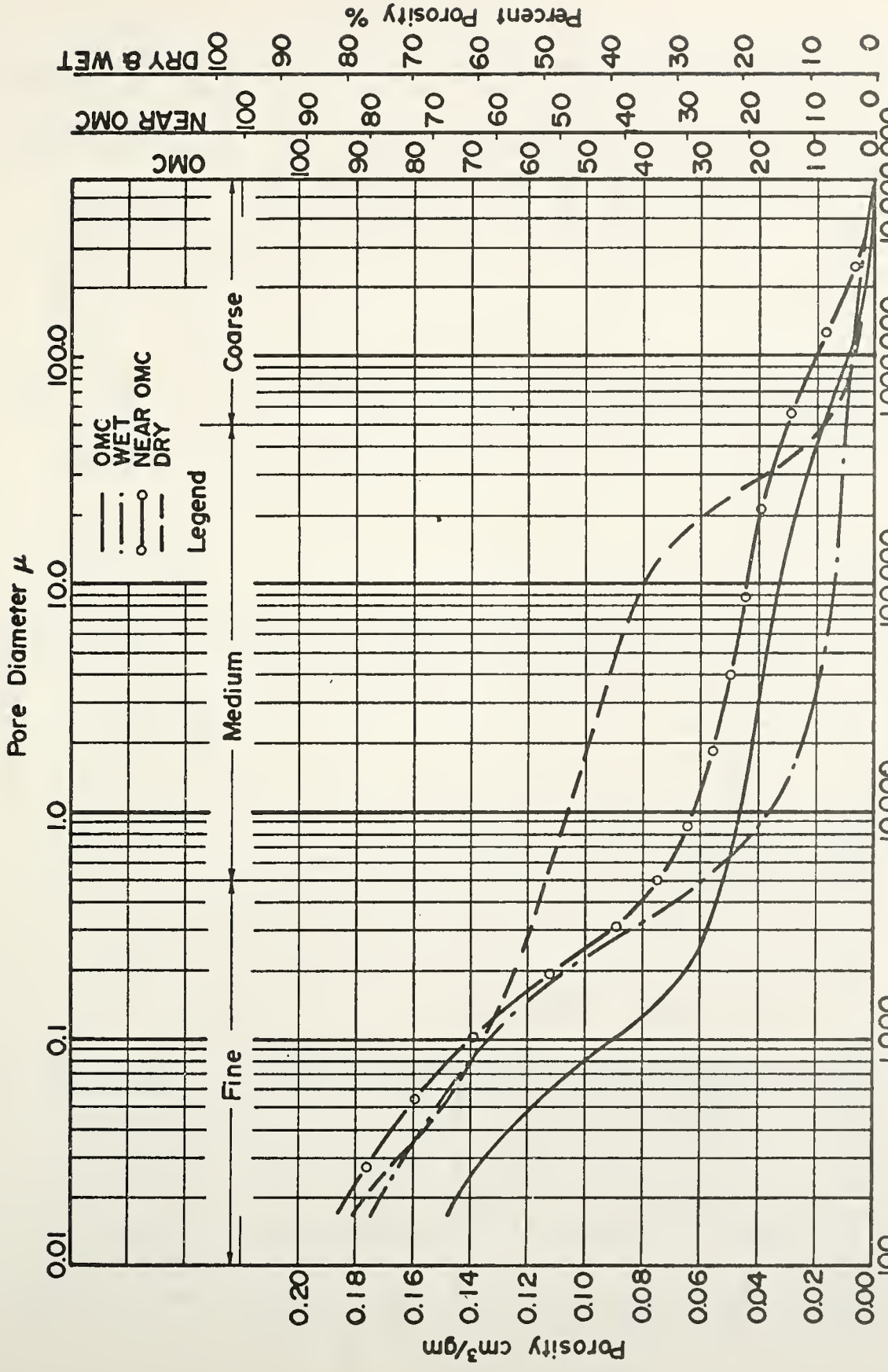

Figure 5. Pore Size Distributions of Samples Compacted by Standard Proctor (SP) at Various Water Contents.

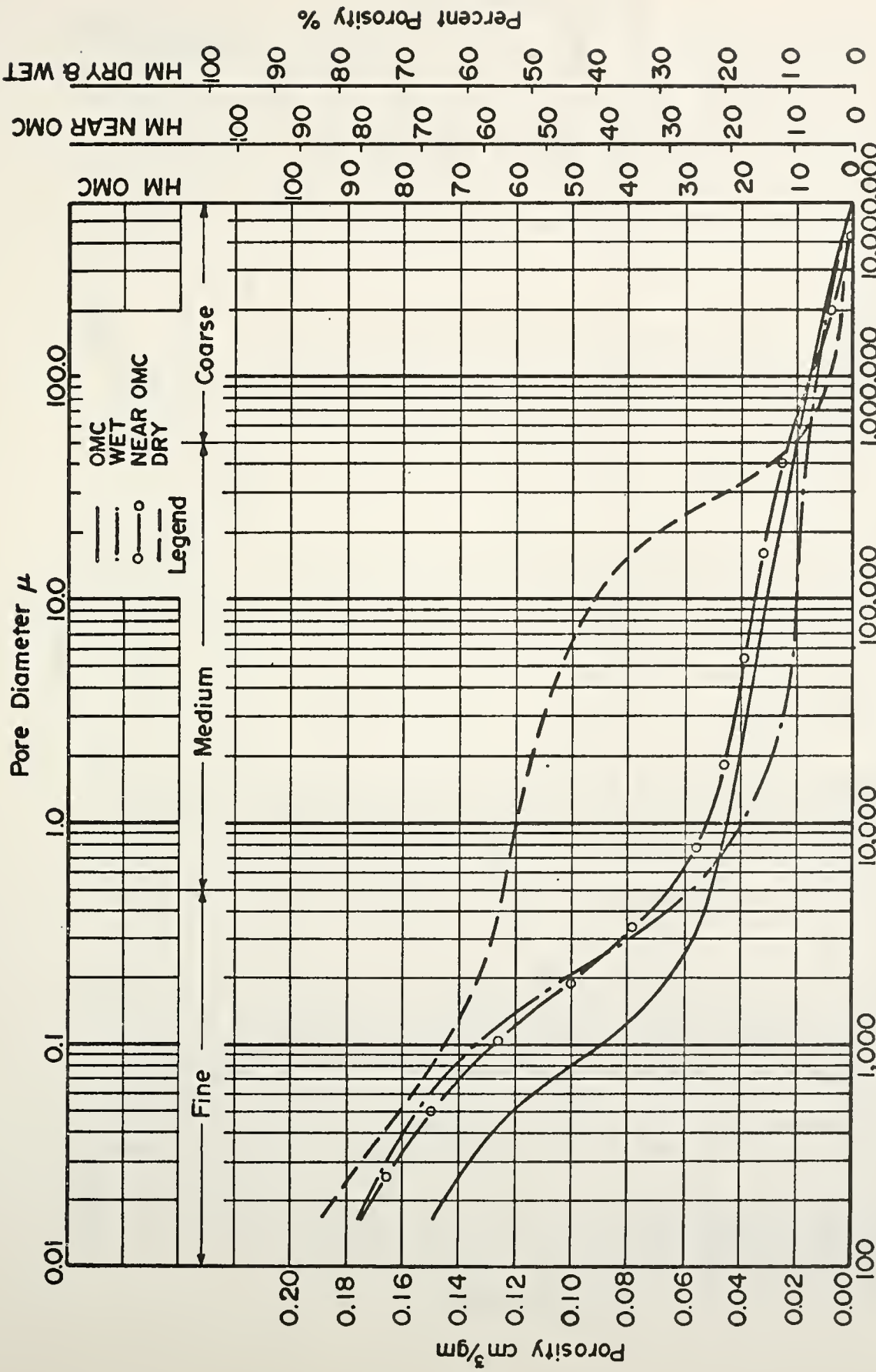

Figure 6. Pore Size Distributions of Samples Compacted by Kneading Compaction (HM) at Various Water Contents.

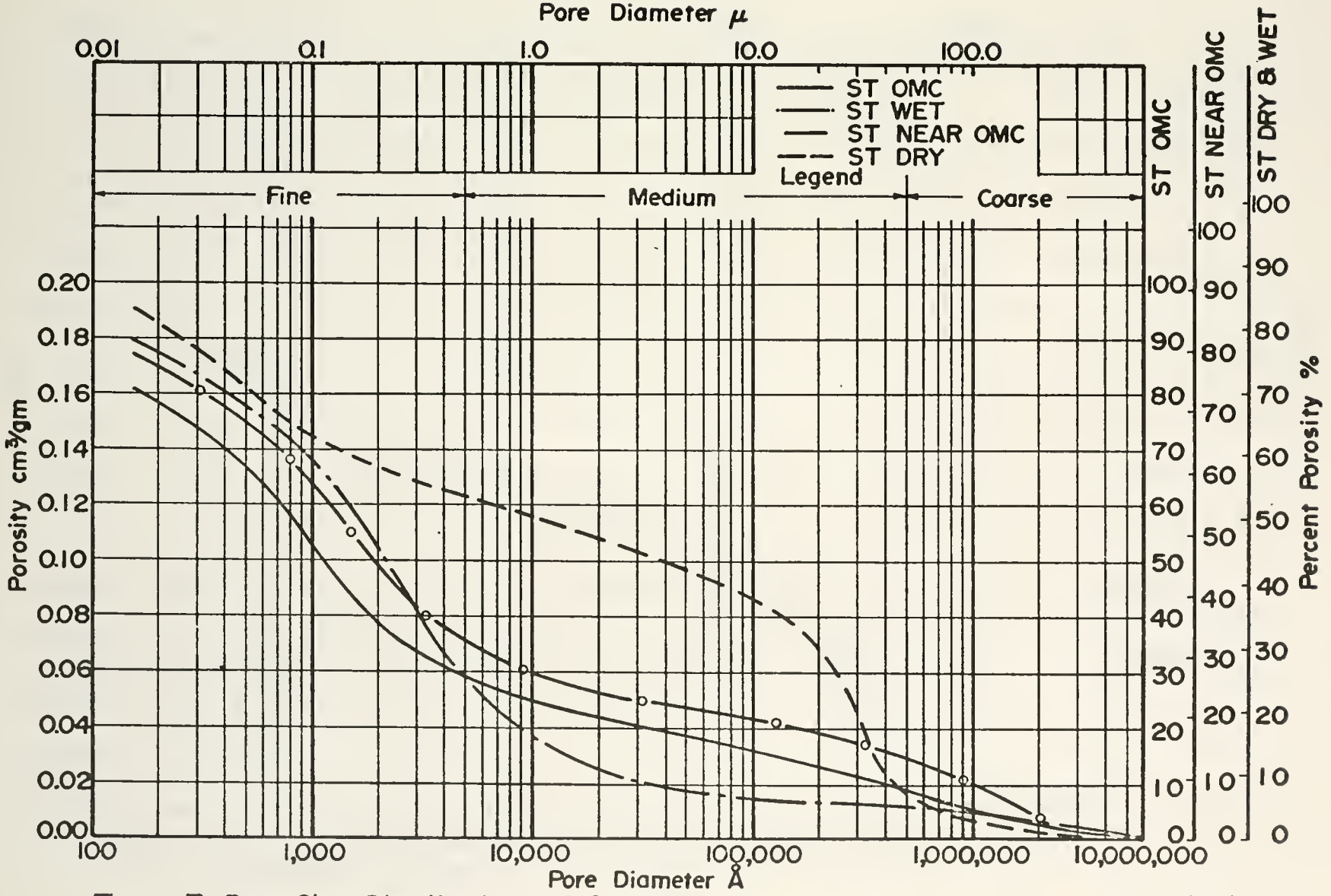

Figure 7. Pore Size Distributions of Samples Compacted by Static Compaction (ST) at Various Water Contents.

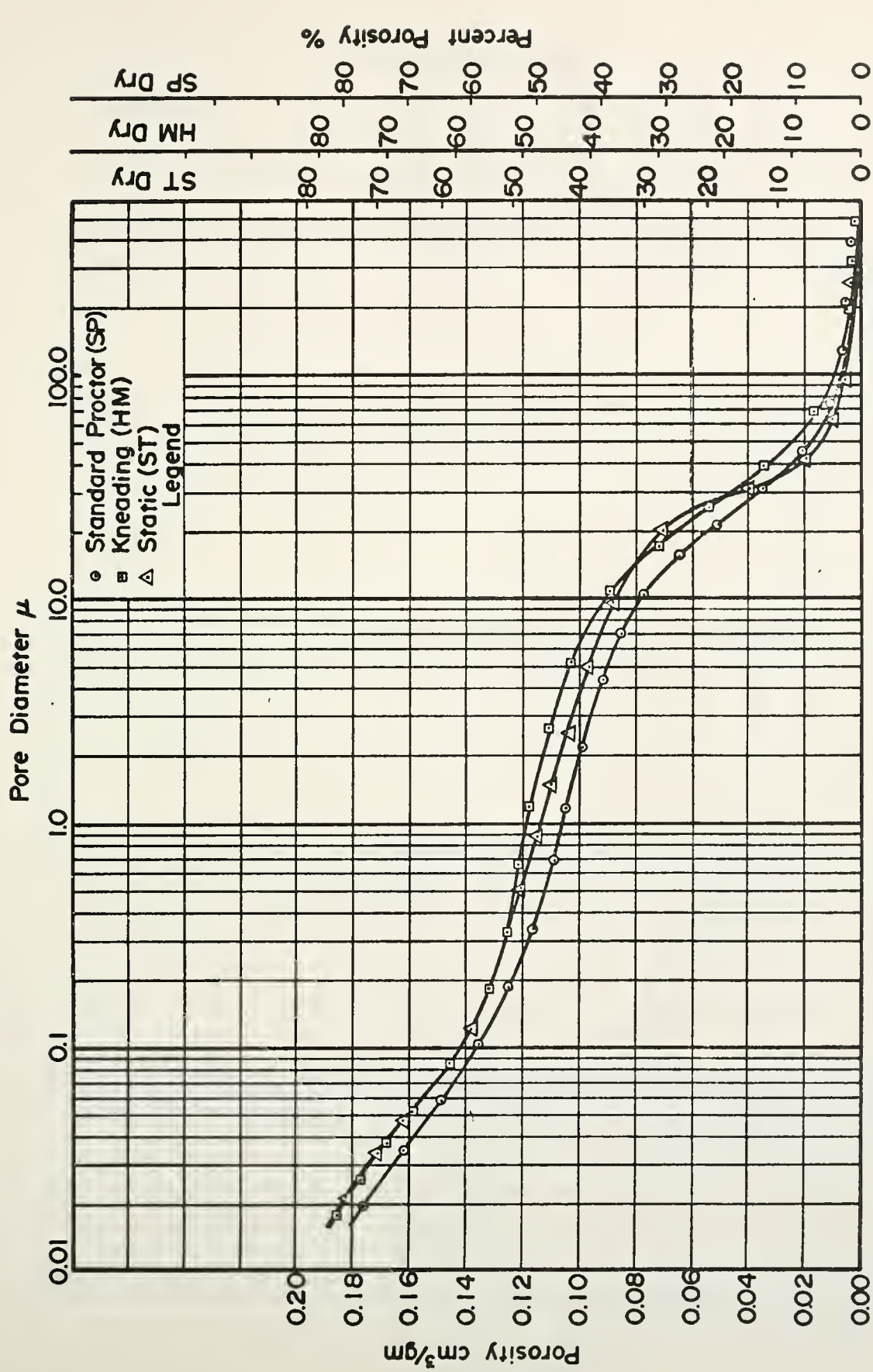

Figure 8. Pore Size Distributions for Compaction on Dry Side by Different Compaction Methods.

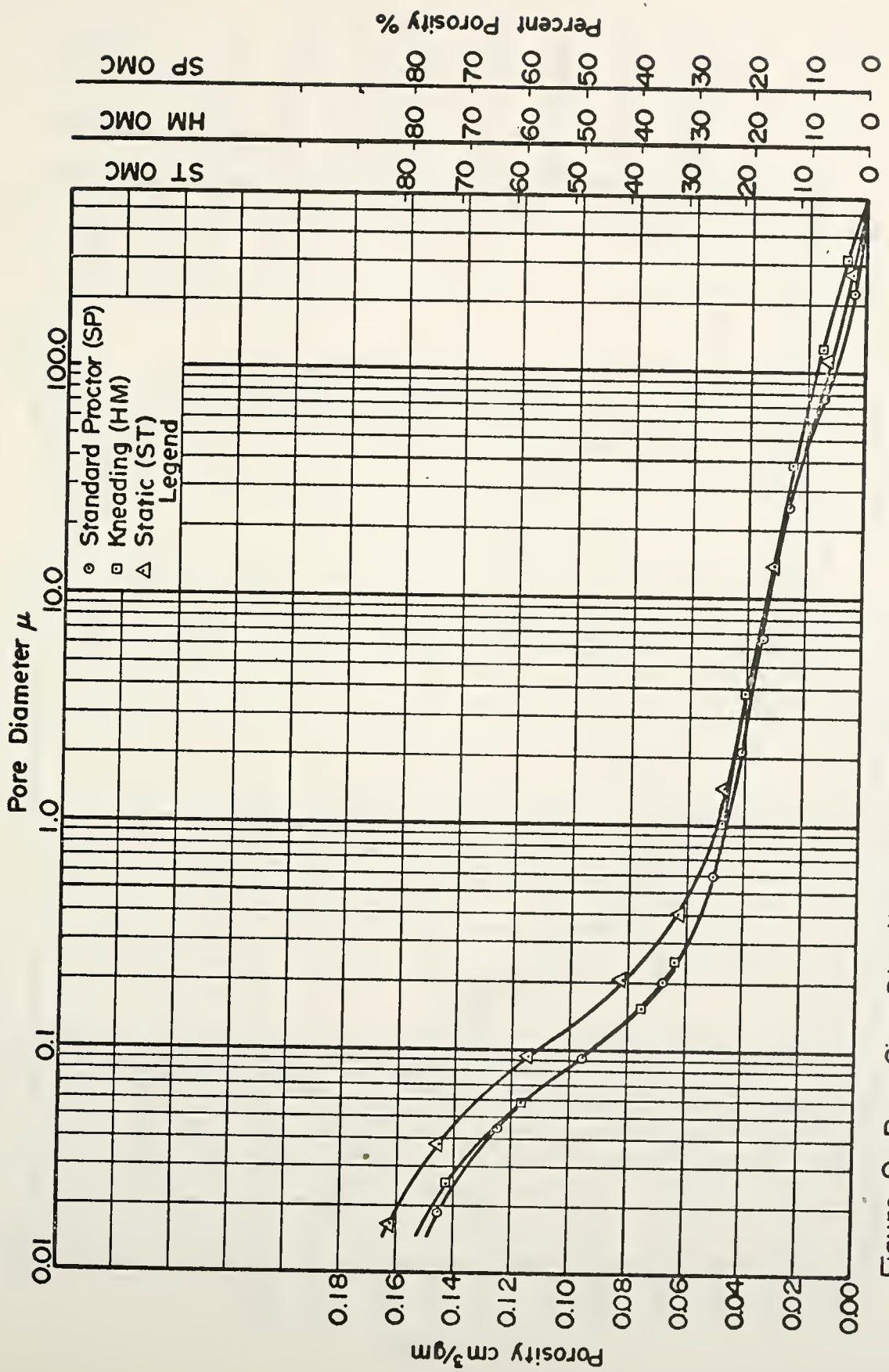

Figure 9. Pore Size Distributions for Compaction at Optimum by Different Compaction Methods.

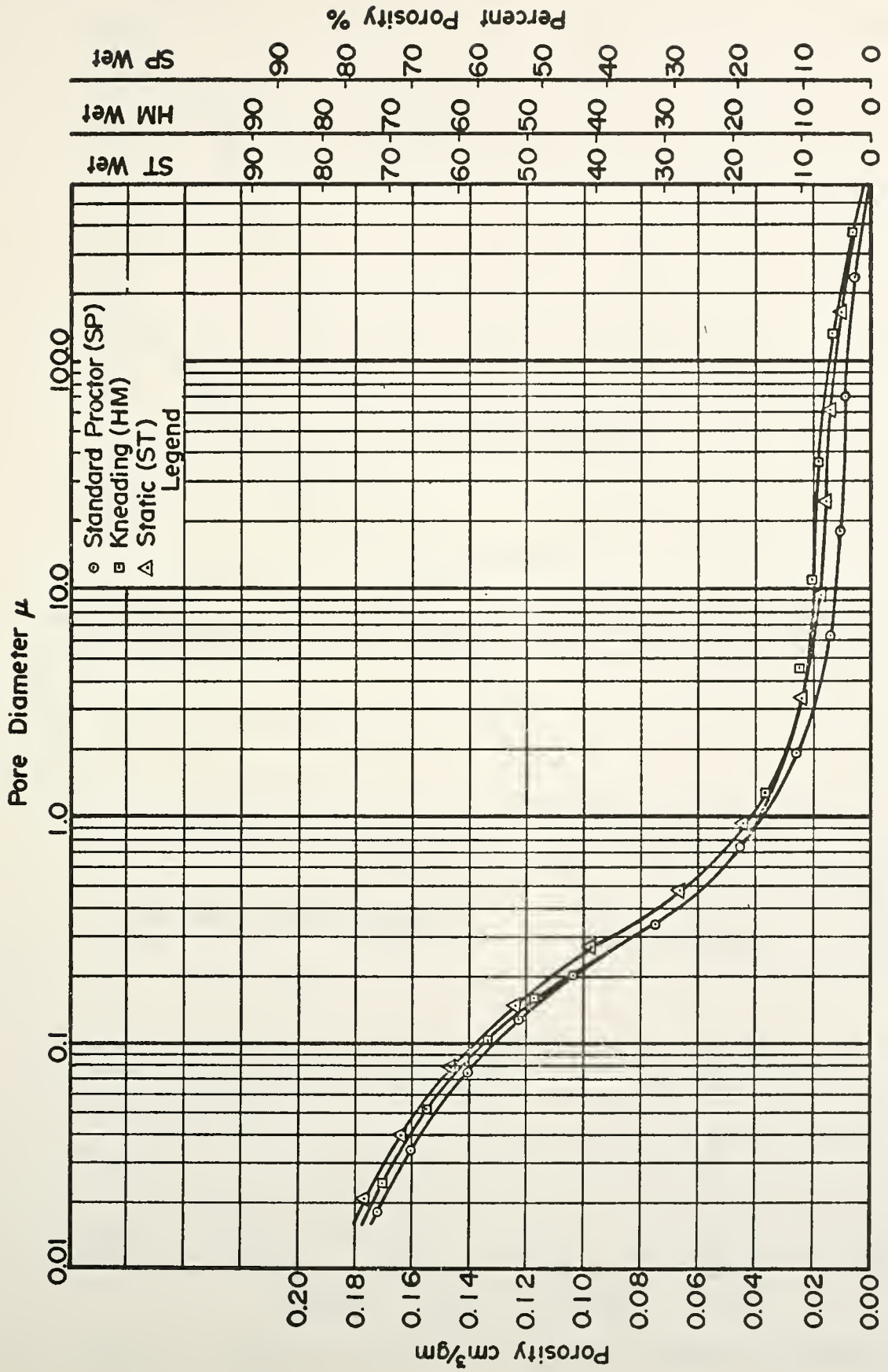

Figure 10. Pore Size Distributions for Compaction on Wet Side by Different Compaction Methods.

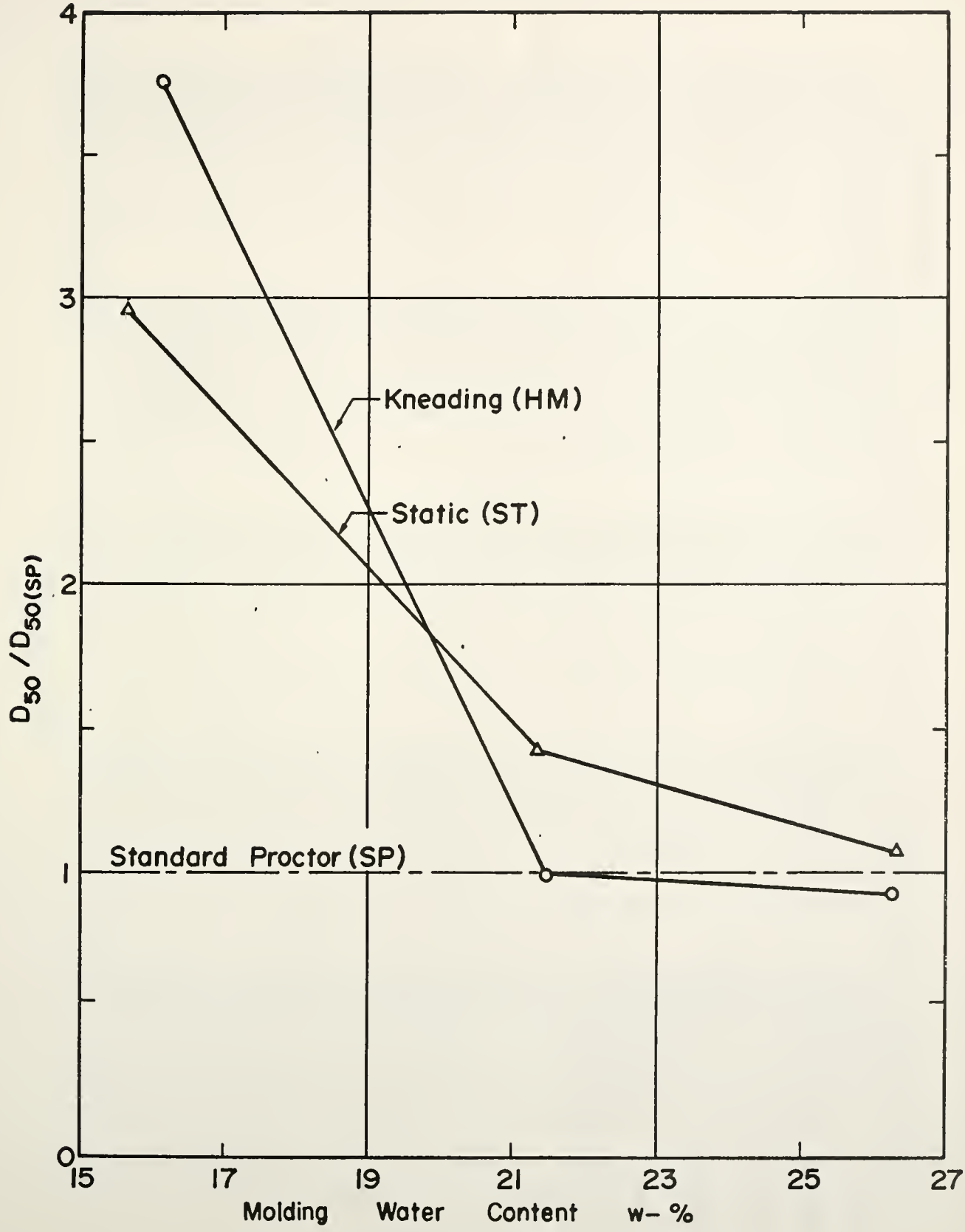

Figure 11. Relative Values of D_{50} for Different Methods of Compaction

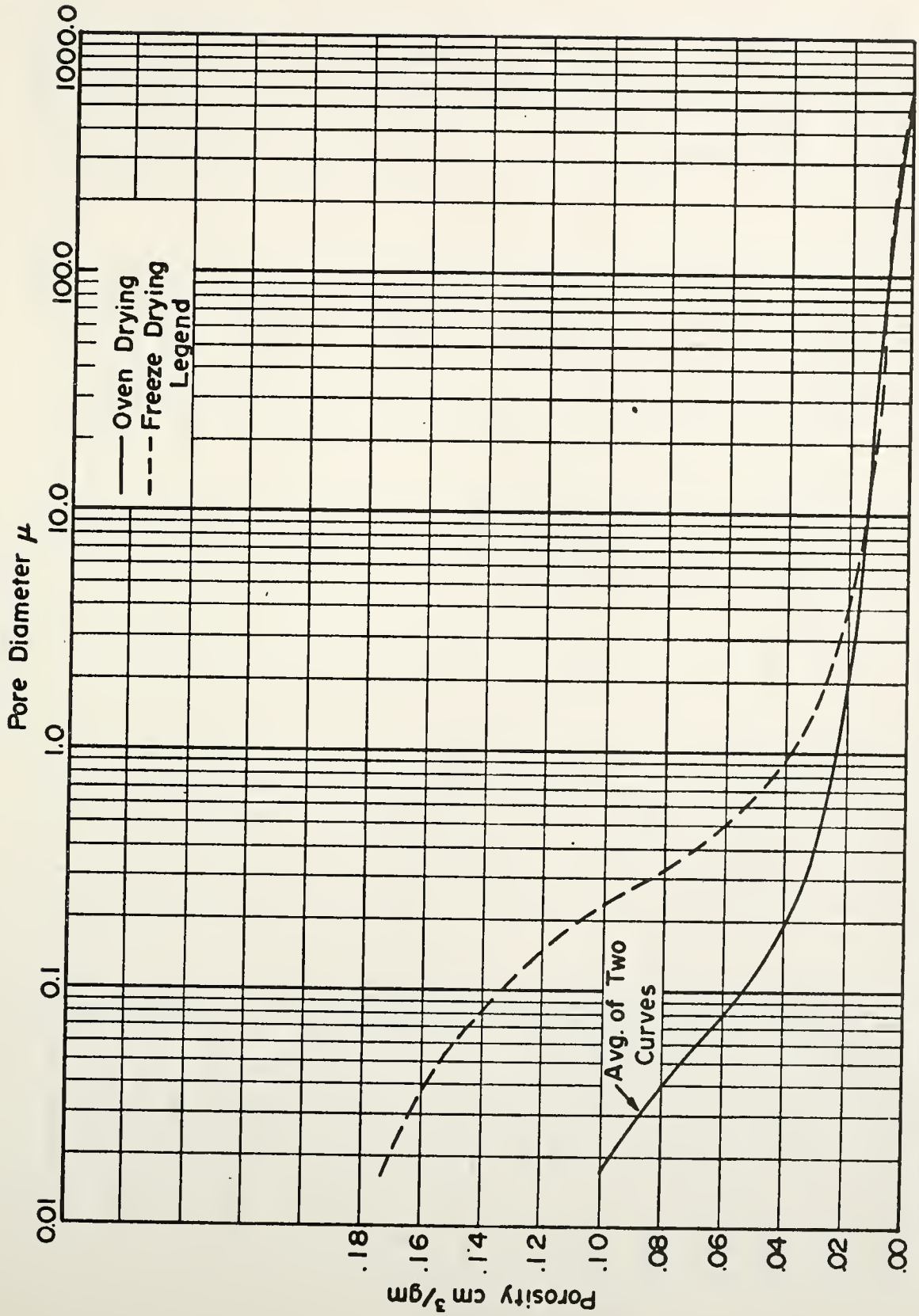

Figure 12. Pore Size Distribution After Oven Drying, Standard Proctor, Wet Side

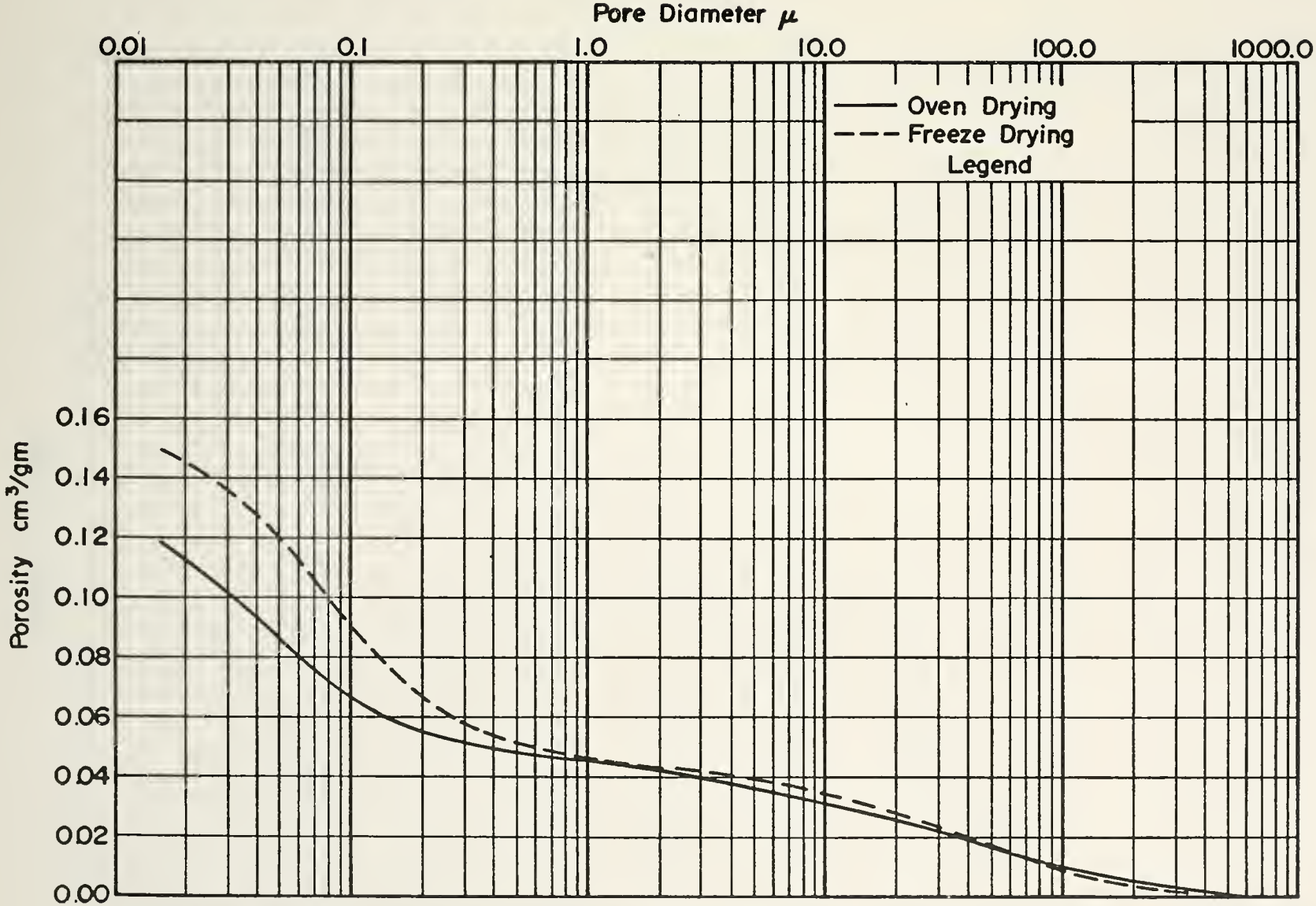

Figure 13. Pore Size Distribution After Oven Drying; Standard Proctor, Optimum

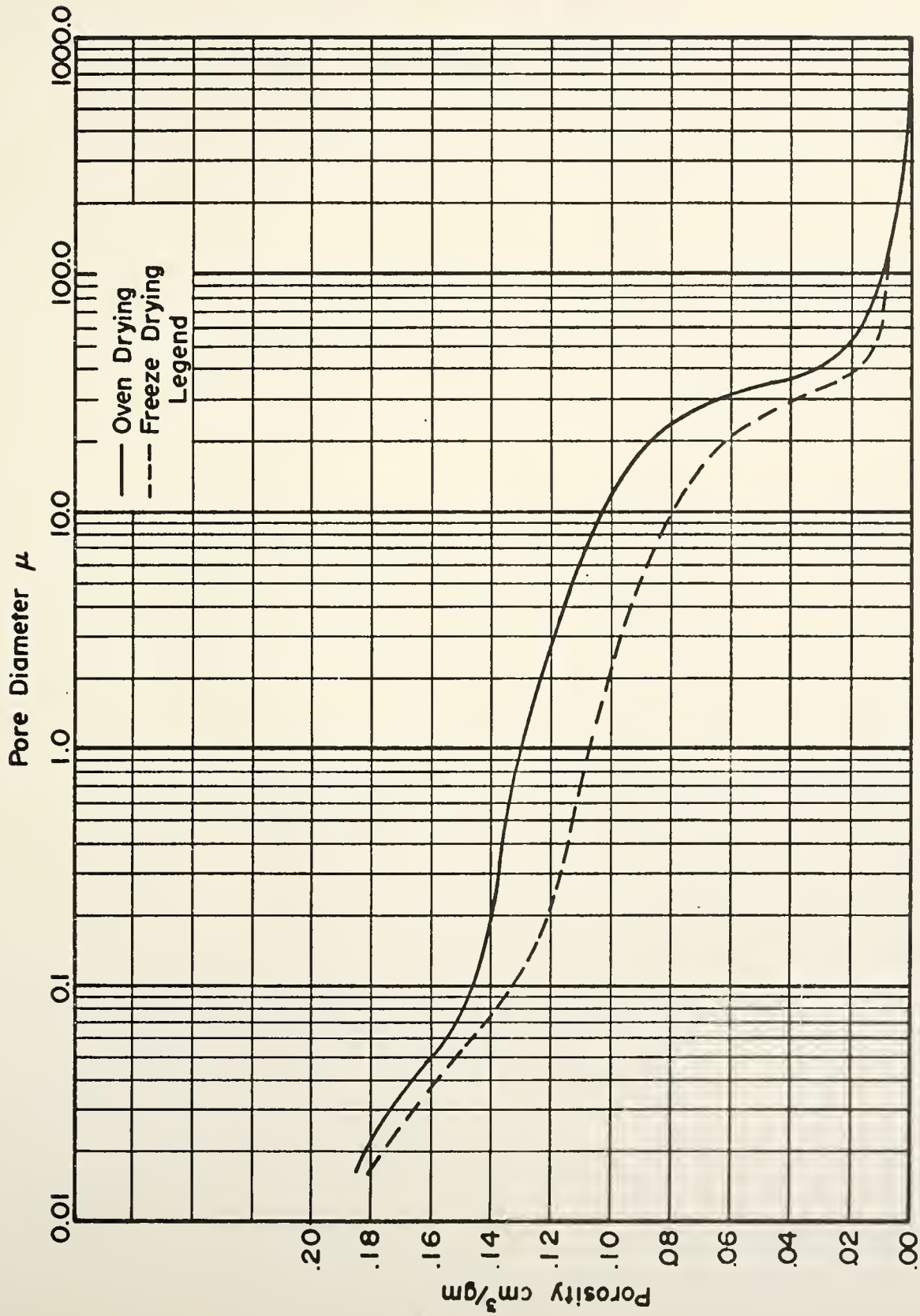

Figure 14. Pore Size Distribution After Oven Drying; Standard Proctor, Dry Side

COVER DESIGN BY ALDO GIORGINI

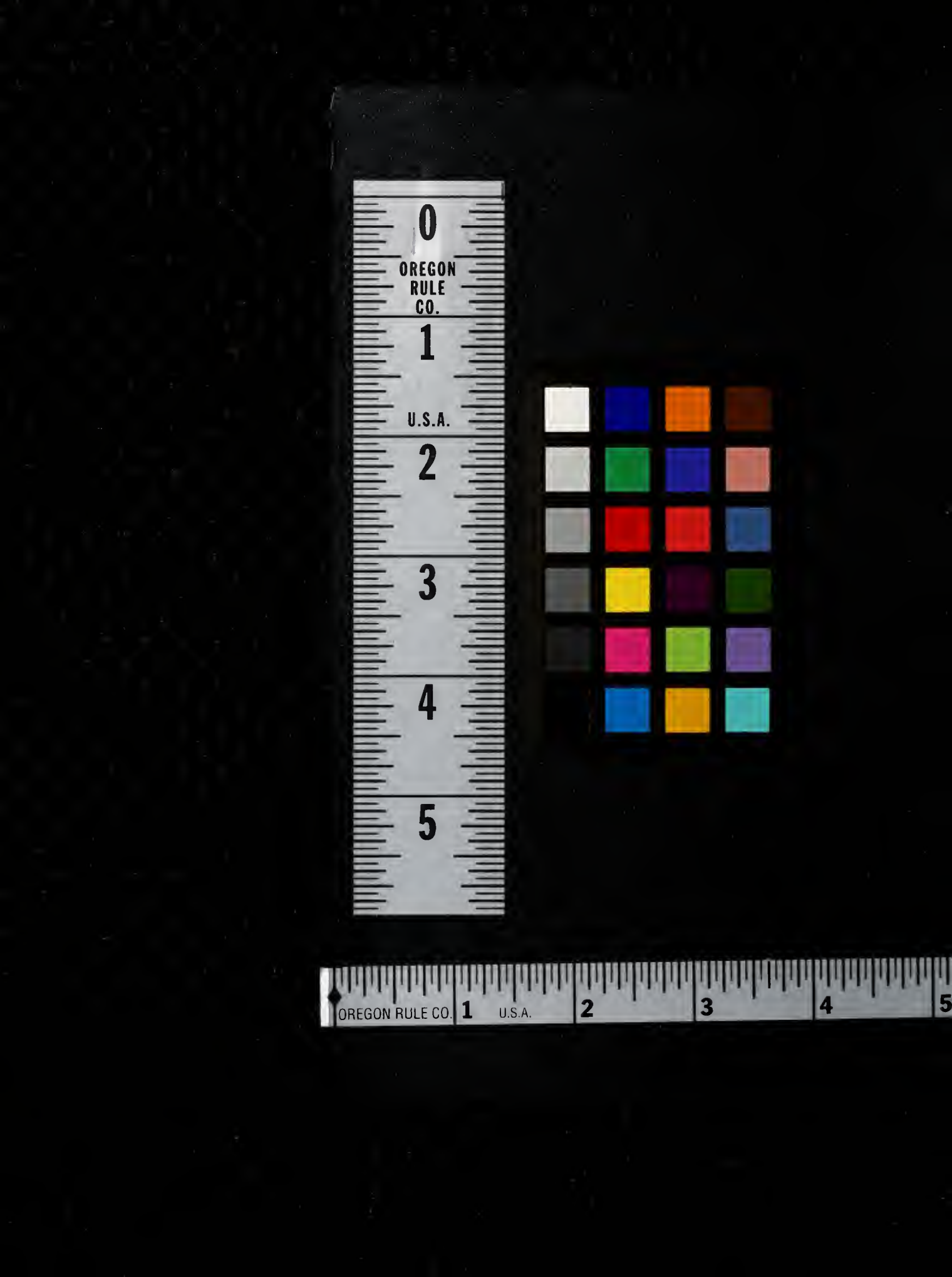
0
OREGON
RULE
CO.
1
U.S.A.
2
3
4
5
OREGON RULE CO.
1
U.S.A.
2
3
4
5

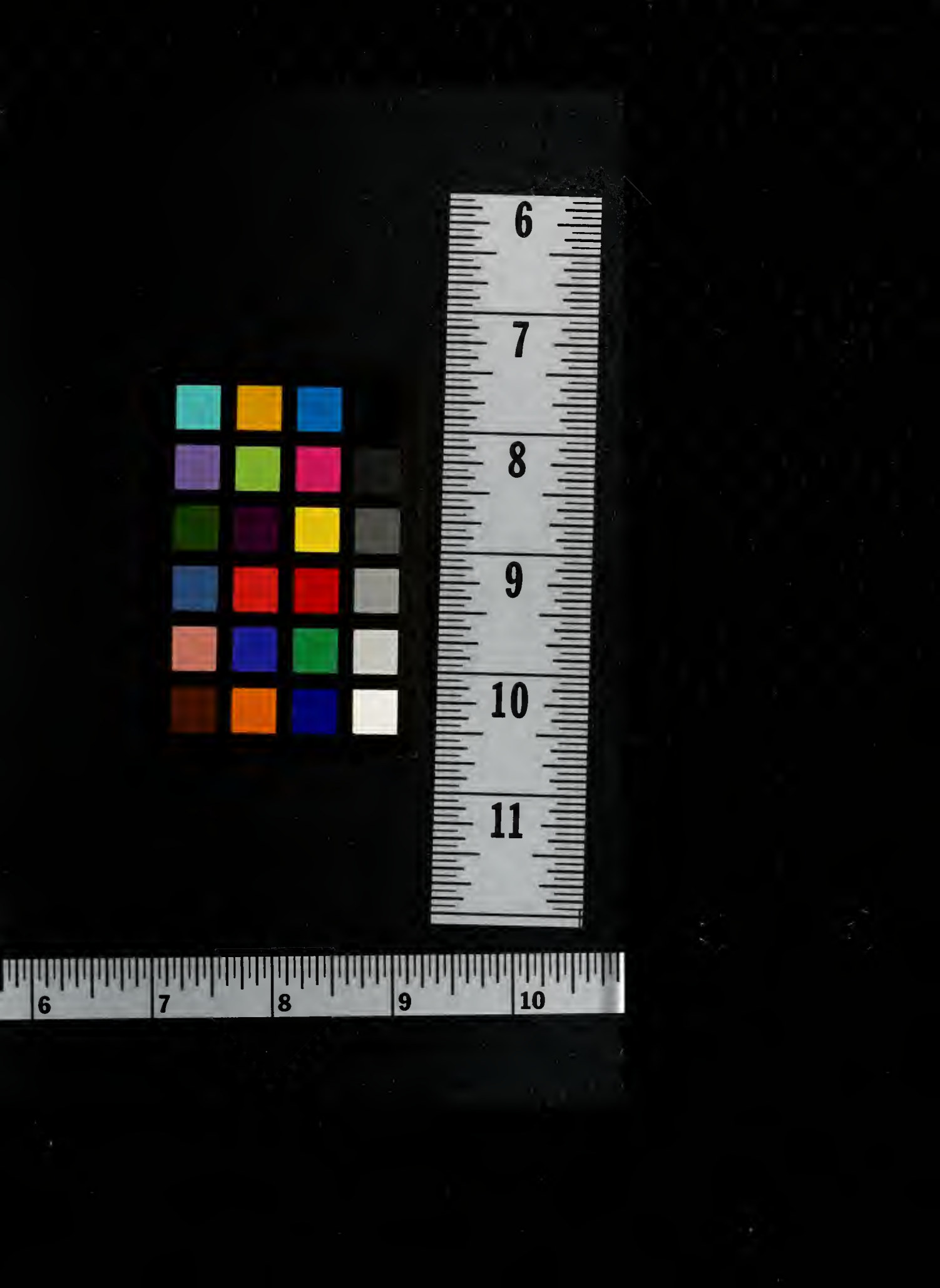
6
7
8
9
10
11
6
7
8
9
10